
Supplementary Material for muSSP: Efficient Minimum-cost Flow Algorithm for Multi-Object Tracking

Anonymous Author(s)

Affiliation

Address

email

1 Proofs of theorems and lemmas in the methods section

2 Any definition, lemma, or theorem is referred to using the same index in the main body and in this
3 supplementary material, if it is discussed in both of them. The major goal of the proofs is to show
4 that with the fundamental changes to the graph or to SSP framework, the optimality of final solution
5 is not influenced.

6 1.1 Independent flipping lemma

Definition 1.1a. The cost associated with a directed path π is

$$\text{pathcost}(\pi) = \begin{cases} \sum_{(u,v) \in \pi} C(u,v) & \text{if } \pi \neq \emptyset \\ \infty & \text{otherwise.} \end{cases}$$

7 **Lemma 1** (Independent flipping). Given a residual graph $G_r(V_r, E_r, C_r)$ and its \mathcal{SP} denoted as T
8 rooted at s , if we flip all edges in path $\pi_T(t)$ and get new graph G'_r , for node $v \in V_r$ that is independent
9 with node t in T , its least-cost path $\pi_T(v)$ is still valid in the new graph, i.e., $\pi_T(v) \in \Pi_{G'_r}^*(s, v)$.

10 *Proof.* Assume there is a new shortest path $\pi_{G'_r}(s, v)$ from s to node v after flipping, which is shorter
11 than $\pi_T(v)$. It is obvious that this path contains flipped edge(s). We can cut $\pi_{G'_r}(v)$ into 4 parts
12 $\{(s, \dots, v_1), (v_1, \dots, v_2), (v_2, \dots, v_3), (v_3, \dots, v)\}$. Part 1 and 3 contain only edges existing in E_r
13 and part 2 contains only flipped edges. Except the 4th part, the other three can not be empty. Because
14 (v_1, \dots, v_2) are flipped edges in T , we have $d_T(v_2) + \text{pathcost}(v_2, \dots, v_1) \leq \text{pathcost}(s, \dots, v_1)$.
15 For the same reason, $d_T(v_3) \leq d_T(v_2) + \text{pathcost}(v_2, \dots, v_3)$. After adding these two inequalities
16 together, we have $d_T(v_3) \leq \text{pathcost}(s, \dots, v_1) - \text{pathcost}(v_2, \dots, v_1) + \text{pathcost}(v_2, \dots, v_3)$,
17 which is $d_T(v_3) \leq d_{G'_r}(v_3)$. If the 4th part is empty, the proof is done. If not, we can further cut
18 (v_2, \dots, v) into 4 parts and continue until the 4th part is empty. Then we can have $d_T(v) \leq d_{G'_r}(v)$,
19 which means $\pi_T(v)$ is still the shortest path in G'_r . \square

20 1.2 Dummy edge clipping

21 **Lemma 2.** No dummy edge will appear in any optimal solution.

22 *Proof.* Assume an optimal solution f^* contains a dummy edge (u, v) , which is in s - t path $\pi =$
23 $\{(s, \dots, u), (u, v), (v, \dots, t)\}$. It is clear that $f_{sv} = f_{ut} = 0$. From the definition of dummy edge,
24 we know that by separating π into two paths $\{(s, \dots, u), (u, t)\}$ and $\{(s, v), (v, \dots, t)\}$, the total
25 cost of f^* can be further decreased. This contradicts the assumption. \square

26 **Theorem 1.** Given a graph $G(V, E, C)$ for MOT, removing all its dummy edges does not influence
 27 the optimality of the final solution.

28 *Proof.* For a min-cost flow problem on a graph G , assume G' is the same graph as G but clipping
 29 all dummy edges. It is clear that the optimal solution $f_{G'}^*$ on G' is a feasible solution on G . For an
 30 optimal solution f_G^* on G , because it does not contain dummy edges, it is also a feasible solution to
 31 G' . Thus, the optimal solutions on G and G' are equivalent. \square

32 1.3 Permanent edge clipping

33 **Lemma 3.** Any s - t path with permanent edge is not a simple path.

34 *Proof.* An s - t path should start at s and end at t . If the path contains an edge that leaves t , it needs to
 35 eventually come back to t , which creates a cycle. The same reasoning applies to the case when the
 36 path contains an edge that go toward s . \square

37 **Lemma 4.** Given a residual graph, we can always find a shortest s - t path which is also a simple path,
 38 unless t cannot be reached from s .

39 *Proof.* Our original graph is DAG with no cycles. Because we only augment flow along the shortest
 40 path in the residual graph, this will never generate negative-cost cycle in residual graph [1]. Removing
 41 cycles in a path will not increase its cost, so for any non-simple s - t path, we can find a simple one at
 42 least as good as it. \square

43 **Theorem 2.** Given a residual graph $G_r(V_r, E_r, C_r)$, removing all its permanent edges does not
 44 influence the optimality of the final solution.

45 *Proof.* Assume this residual graph G_r is generated in iteration i and we totally need K iterations.
 46 We first prove that the i th iteration to K th iteration in SSP, it is equivalent to solve a new min-cost
 47 flow problem with excess flow number $K - i + 1$ on G_r . This is obvious from the paradigm of SSP
 48 algorithm. Now we prove that for the new min-cost flow problem, removing permanent edges does
 49 not influence the optimality of the final solution. We denote the graph without permanent edges as
 50 $G_{r \setminus p}$. From lemma 3 and 4, we know that we can have at least one optimal solution f^* to the new
 51 min-cost flow problem on G_r with only simple paths. Assume the optimal solution on $G_{r \setminus p}$ is f^o if
 52 there is one. It is clear that f^o is a feasible solution to G_r , and we have $C_r * f^o \geq C_r * f^*$. Because
 53 f^* contains no permanent edges, f^* is also a feasible solution for $G_{r \setminus p}$ and $C_r * f^o \leq C_r * f^*$. Then
 54 we get $C_r * f^o = C_r * f^*$, so the optimality are not influenced. \square

55 1.4 Multi-path finding

56 **Lemma 5.** Given a residual graph $G_r(V_r, E_r, C_r)$, its \mathcal{SP} rooted at s , and the shortest distance
 57 function d from s to each node, we have $d(t) = \min(d(v) + d_t(v)), v \in V_r \setminus \{t\}$.

58 *Proof.* For any s - t path $\pi = \{(s, \dots, v_x), (v_x, t)\}$, $\text{pathcost}(\pi) \geq d(v_x) + d_t(v_x)$. Thus we have
 59 $d(t) \geq \min(d(v) + d_t(v)), v \in V_r$. Based on the definition of shortest path and $d_t(v)$, we have
 60 $d(t) \leq d(v) + d_t(v)$, for any $v \in V_r$. Thus $d(t) = \min(d(v) + d_t(v)), v \in V_r \setminus \{t\}$. \square

61 By maintaining a sorted list $\{d(v) + d_t(v)\}$ in ascending order, we can directly extract the shortest
 62 s - t path by popping the top element in the list. The updating of sink t after path flipping can also be
 63 fulfilled by updating this list.

64 **Lemma 1.4a.** Given a graph $G(V, E, C)$ with source node s and sink node t , and its \mathcal{SP} T rooted at
 65 s with shortest distance function d , flipping the shortest s - t path will never decrease distance $d(v)$ in
 66 the new graph, for any $v \in V$.

67 *Proof.* The proof is similar to lemma 1. From lemma 1, we know this is true for nodes that
 68 independent with node t . Here we only consider nodes that inside the same branch with t . Assume
 69 the graph with flipped path is G_r . There is a new shortest path $\pi_{G_r}(v)$ in G_r , from s to node v , whose
 70 cost is smaller than $\pi_T(v)$. It is obvious that this path contains flipped edge(s). We can cut $\pi_{G_r}(v)$

71 into 3 parts $\{(s, \dots, v_1), (v_1, \dots, v_2), (v_2, \dots, v)\}$. Part 1 contains only edges existing in E and part
72 2 contains only flipped edges. Part 1 can not be empty. If part 2 and 3 are empty, the lemma is correct.
73 If part 2 is not empty, from $SP T$, we have $d_T(v_2) + \text{pathcost}(v_2, \dots, v_1) \leq \text{pathcost}(s, \dots, v_1)$,
74 which means $d_T(v_2) \leq d_{G_r}(v_2)$. If part 3 is empty, $v_2 = v$, the proof is done. If part 3 is not empty
75 but contains no flipped edges, we have $d_T(v_2) + \text{pathcost}(v_2, \dots, v) \geq d_{T(v)}$. After adding the
76 previous inequality together, we have $d_T(v) \leq d_{G_r}(v)$. If part 3 is not empty and contains flipped
77 edges, we can continue previous cutting strategy on part 3 until the new part 3 is empty or contains
78 no flipped edges. Then we can have $d_T(v) \leq d_{G_r}(v)$, which means the cost of the new shortest path
79 does not decrease. \square

80 This lemma shows that every time when we find a shortest s - t path, flipping it will not create a shorter
81 path in the residual graph. Before flipping the shortest path, the node occupying the top of the sorted
82 list $\{d(v) + d_t(v)\}$ denotes current shortest path that should be instantiated. After flipping, the top
83 element is popped out. After that, if the new top node of the list is independent with the popped
84 one, it will hold that position and become the next shortest path to be flipped. Based on the same
85 reasoning. We can generalize this reasoning in the following theorem.

86 **Theorem 3.** Given a residual graph $G_r(V_r, E_r, C_r)$, its SP denoted as $T(V_r', E_r', C_r)$ rooted
87 at s and a sorted list of $\{d(v) + d_t(v)\}$ with $v \in V_r$ with ascending order, if the k nodes
88 $\{v_1, v_2, \dots, v_k\}$ that occupy the top k locations of the list are mutually independent, the k paths
89 $\{\pi_T(v_1), \pi_T(v_2), \dots, \pi_T(v_k)\}$ can be simultaneously instantiated as k shortest paths.

90 *Proof.* From lemma 5, we know v_1 indicates current shortest path π_1 . We only need to prove that for
91 any $i \in \{1, \dots, k\}$, after popping the nodes $\{v_1, \dots, v_i\}$ in the list, the $i + 1$ node will occupy the
92 top of the list. Because the k nodes are mutually independent, v_{i+1} is independent with $\{v_1, \dots, v_i\}$.
93 From lemma 1, we know $d(v_{i+1})$ does not change in the residual graph after i iterations. From
94 lemma 1.4a, we know $d(u)$ does not decrease for any $u \in V_r$, so after popping out $\{v_1, \dots, v_i\}$, in
95 the new graph v_{i+1} will occupy the top location of the list and indicate the new shortest path. \square

96 1.5 Batch updating and heap shrinking

97 **Lemma 6.** Given a 0-tree $T_0(V_0, E_0, C_r)$ embedded in residual graph $G_r(V_r, E_r, C_r)$, if $v \in$
98 $\text{descendants}(v_0)$, $d_u^*(v) \leq d_u^*(v_0)$, $\forall u \in V_r, \forall v_0 \in V_0$.

99 *Proof.* Because $v \in \text{descendants}(v_0)$, there is a path from v to v_0 in T_0 with only 0-cost edges. Thus
100 $d_u^*(v) \leq d_u^*(v_0)$, $\forall u \in V_r, \forall v_0 \in V_0$. \square

101 **Theorem 4.** In Dijkstra's algorithm, if the distance from s to a node v in a 0-tree is permanently
102 labeled as $d(v)$, $d(v)$ is also the permanent label for the nodes in $\text{descendants}(v)$ that haven't been
103 permanently labeled.

104 *Proof.* Based on the property of Dijkstra's algorithm, for a permanently labeled node v , its distance
105 $d(v) \leq d(u)$ for any node u with temporary label. If $u \in \text{descendants}(v)$, $d(v) \geq d(u)$ based on
106 lemma 6. Thus, we can permanently label node u as $d(v)$. \square

107 **Lemma 7.** In a 0-tree, nodes with larger temporary distance labels than their parent belong to set P .

108 *Proof.* The temporary distance of a node v is from the relaxation of edges linked from nodes outside
109 of the 0-tree. If it is larger than the temporary distance label of its parent node u , based on lemma
110 6, v will be updated at least once more by relaxing edge (u, v) . Thus v cannot be correctly labeled
111 without checking nodes in the 0-tree. \square

112 2 Complexity analysis

113 2.1 Time complexity analysis

114 Min-cost flow in MOT problem can be solved by successive shortest path (SSP) algorithm with
115 computational complexity $O(K(n \log(n) + m))$ [7], where n and m are the number of vertices
116 and arcs, respectively. We now show that the complexity of muSSP algorithm does not increase

117 compared with SSP. The complexity of graph cleaning and finding the shortest path in DAG is
118 $O(m)$, which only run once. The loop will terminate with K iterations. For one iteration, identifying
119 the nodes to update takes $O(n)$ operation by checking their branch nodes. Finding multi-paths for
120 flipping can be efficiently done by maintaining the list mentioned in section 3.5. The list can be
121 implemented by priority queue with updating complexity $O(n \log(n))$. Converting edge costs takes
122 $O(m)$ time, while building residual graph and clipping permanent edges take amortized constant
123 time. The best complexity for implementing Dijkstra's algorithm is $O(n \log(n) + m)$. Consequently,
124 the complexity in one iteration is still dominated by Dijkstra's algorithm as $O(n \log(n) + m)$ and the
125 overall complexity is $O(K(n \log(n) + m))$. The worst case for muSSP happens when the shortest-
126 path tree contains only one branch in each iteration of Alg. 1. This worst case is unlikely to happen
127 in the graph of MOT problem, as the number of branches is at least equal to the number of objects in
128 the first (or last) frame of the video.

129 2.2 Space complexity analysis

130 The efficiency improvement is achieved without sacrificing memory cost. Given a graph with the
131 number of nodes n and number of edges m , the memory consumption for the graph itself is $O(m+n)$.
132 Dummy edge clipping and permanent edge clipping use $O(1)$ space. For each node, we save a branch
133 node label, parent node label, distance label of each node which need $O(n)$ space. The list and
134 heap used in Dijkstra algorithm in multi-path flipping also need $O(n)$ space. Thus our memory
135 consumption is totally $O(m+n)$, which is the same as SSP and FollowMe[6].

136 3 Experiments

137 3.1 Effectiveness of each individual strategy

138 For different graphs, the contribution of these strategies incorporated in muSSP varies significantly.
139 First, we check the number of nodes updated in each iteration, and Fig.1 shows the comparison
140 of our first three strategies and the other methods on the two sample graphs. Details of the graphs
141 can be found in the caption of the figure. "DC" and "PC" are short for "dummy-edge clipping" and
142 "permanent-edge clipping", and "DC-PC" represents these two strategies are applied simultaneously.
143 We can see that by clipping dummy/permanent edges, the number of nodes to update dramatically
144 decreases compared with FollowMe or SSP. Because SSP can have an early stop once it finds the
145 shortest $s-t$ path [1], the updated number of nodes is not necessarily to be the same as node number
146 in the graph. In fig.1a, we did not show the result of "DC-PC", because in this graph, there is no
147 dummy edge. DC will not contribute to decrease the number of nodes for updating. However, in
148 fig.1b, there is a clear difference between curve "PC" and "DC-PC" especially in the early iterations.
149 Purple spikes denote the iterations updating is really conducted. Gaps between purple spikes mean
150 we find those shortest $s-t$ paths without updating the shortest path tree. After applying multi-path
151 flipping, the number of updating shortest path tree decreases from 470 to 123 in the graph used in
152 fig.1a and 466 to 106 in the graph used in fig.1b.

153 Using the same graph as fig.1a, we show the power of batch updating (BU) and heap shrinking (HS)
154 in table 1. Here "muSSP" incorporates the first 3 strategies. "muSSP-BP" includes the batch updating
155 and "muSSP-BU-HS" includes both the batch updating and heap shrinking. The heap we are using
156 are based on binary search trees, which has amortized constant complexity for popping and $\log(n)$
157 for pushing. Thus, the heap operation here only considers pushing operation. Clearly, purely with the
158 first 3 strategies, the number of nodes for updating has already significantly decreased. With batch
159 updating, the number of heap operations decreases for one more order. The initial heap size can also
160 be decreased to half with heap shrinking. Here we do not consider the number of heap operations in
161 building the initial heap because for SSP, it is always 1. FollowMe indeed suffers a lot from the initial
162 heap size. They insert every node in the previously flipped path to the heap first. This operation will
163 make the heap huge when we have a large number of paths.

164 3.2 Implementation details

165 Except for cs2, muSSP, SSP, and FollowMe are all implemented in C++. The source code of these
166 3 algorithms can be found on GitHub(<https://github.com/yu-lab-vt/muSSP>). We use
167 the data structure of self-balanced binary search tree to implement the Dijkstra's algorithm which

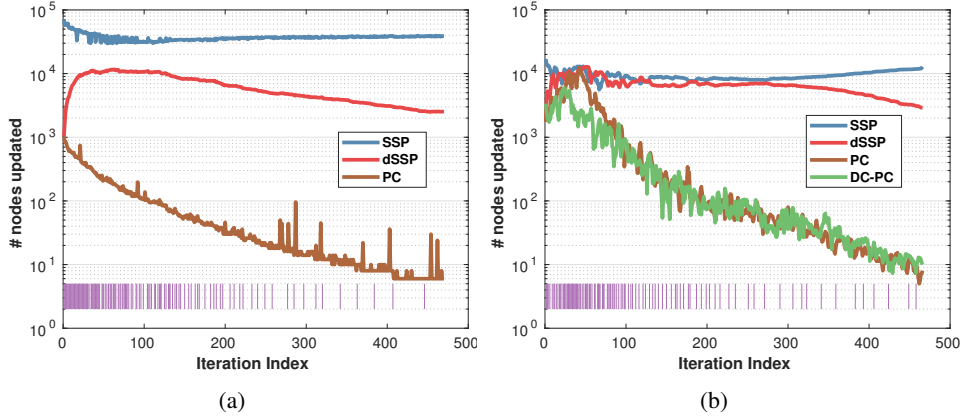


Figure 1: The effectiveness of dummy-edge clipping ("DC"), permanent-clipping ("PC") and multi-path flipping on two different graphs. Gaps between purple spikes denote the iterations we skipped because of multi-path flipping. The graph used in (a) is from sequence 07 in MOT CVPR19 dataset with graph design method in [6]. The graph in (b) is from ISBI12 Particle Tracking Challenge (sequence name: "RECEPTOR snr 7 density low") with probability principled graph design described in supplementary.

Table 1: Comparison of # heap operation and initial heap size

Avg. of all iterations	SSP	FollowMe	muSSP	muSSP-BU	muSSP-BU-HS
#Heap operation	44889.5	6225.1	49.6	5.8	5.7
Initial heap size	1.0	33273.9	85.4	85.4	39.4

168 has $O(1)$ for popping top element and $O(\log(n))$ for pushing a new value. This is the reason why
 169 we mainly compare pushing operation number used in Dijkstra's algorithm when testing the fourth
 170 strategy.

171 For muSSP, SSP and FollowMe, it is not needed to explicitly set flow number. For cs2, we use binary
 172 search to find the best flow number as did in [11, 7].

173 Except for cs2, the other 3 methods accept real-valued edge cost and saved using "double" data type.
 174 For cs2, we round the edge costs with accuracy to $1e-7$. More details about implementation can be
 175 found in the attached source code. The cs2 package can be found on the author's website [4].

176 All comparisons were conducted on Ubuntu 16.04 LTS, compiled by g++ v5.4.0 with single core of
 177 2.40GHz Xeon(R) CPU E5-2630 and memory speed at 2133MHz.

178 3.3 Detection results used for graph building

179 For KITTI-Car dataset, we chose four long sequences (seq00, seq10, seq11, seq14) for a clear
 180 efficiency comparison. For sequences that too small, there is no need to speed up for any solver.
 181 KITTI provides two detection results DPM[3] and reglets[10]. We test on both of them. For MOT
 182 CVPR 2019 dataset, we use its test set with 4 videos. Each video contains a crowd of pedestrians.
 183 The detection results are provided by their website. The detection results of ETHZ (BAHNHOF and
 184 JELMOLI) dataset is also DPM from [7]. Particle tracking challenge provided two different types of
 185 simulated particle tracking data: RECEPTOR and VESICLE, each of them contains 15 data with
 186 different signal to noise ratio and particle density. We test our efficiency on the RECEPTOR snr 7
 187 with density from low to high. As this dataset does not provide detection results, we directly use the
 188 ground truth as input to build the graph. The data RECEPTOR snr 4 was used as training data.

189 For the quadratic programming problem, we directly use the function formulated in the published
 190 software package [2]. We use Frank-Wolfe algorithm to approximate the solution. The step size is set
 191 as $k/(k+2)$, where k is the index of the current iteration. We set a stringent stopping criterion and
 192 with max iteration number as 400.

Table 2: Details of KITTI-Car dataset

Datasets	KITTI(DPM)				KITTI(reglets)			
	seq00	seq10	seq11	seq14	seq00	seq10	seq11	seq14
#frames	465	1176	774	850	465	1176	774	850
#detections	51100	181132	104748	96974	19885	22189	24524	35198
(a) graph design from [7]								
#vertices	102202	362266	209498	193950	39772	44380	49050	70398
#arcs	171135	608881	349869	325256	71730	78273	86864	123008
(b) graph design from [6]								
#vertices	102202	362266	209498	193950	39772	44380	49050	70398
#arcs	173242	609576	352140	328352	71977	78524	87048	122875
(c) graph design from [8]								
#vertices	102202	362266	209498	193950	39772	44380	49050	70398
#arcs	172317	607035	350276	326635	71592	78477	86830	122763

Table 3: Details of CVPR19, EHTZ and PTC datasets

Datasets	CVPR19				ETHZ		PTC		
	seq04	seq06	seq07	seq08	seq03	seq04	High	Mid	Low
#frames	2080	1008	585	806	1000	936	101	101	101
#detections	208000	70189	20220	43444	101180	94054	77352	39215	7438
(a) graph design from [7]							probability principled		
#vertices	416002	140380	40442	86890	202362	188110	154706	78432	14878
#arcs	1007552	334881	98255	206836	358546	365461	462213	234438	44448
(b) graph design from [6]									
#vertices	416002	140380	40442	86890	202362	188110			
#arcs	1007436	334513	98256	206557	411170	368080			

193 3.4 Graph design

194 We use three existing methods [7, 6, 8] to build the graph. Details can be found in their paper and
 195 published software packages. [7, 6] are purposely designed with the min-cost flow framework. For
 196 [8], in their package, they design similarity between detections and use Hungarian algorithm [5] to
 197 solve the association problem in every two consecutive frames. The cost they used is just the negative
 198 values of the similarities. We use the same way for linking cost between detections. In [8], they
 199 believe in detection results and majority of the detections have links in adjacent frames. Following
 200 the same thinking, we set the transition edge between the pre-node and the post-node of one detection
 201 as zero. The enter/exit costs are set as a small value to avoid trivial solutions. To tackle the problem
 202 of occlusion or missed detection, for all these datasets, we allow the objects to have one "jump",
 203 which means we allow the objects in frame k to be linked to objects in frames $k + 1$ and $k + 2$.

204 For PTC dataset, we use the ground truth as input. Because particles can suddenly appear or disappear
 205 in the filed of view, we set the cost of $C(s, v) = -\log(p_{enter})$ and $C(u, t) = -\log(p_{exit})$ for
 206 any pre-node v and post-node u . The probabilities p_{enter} and p_{exit} are learned from another data
 207 provided in the challenge (the data "RECEPTOR snr 4"). Because we are using the groundtruth
 208 as input, we set the linkage cost between the pre-node v_i and post-node u_i of the same object
 209 as $C(v_i, u_i) = -(C(s, v_i) + C(u_i, t))$ to make sure the final results will not miss any detection.
 210 The linkage costs between different objects are decided by their distance as we do not have much
 211 appearance features to use as in natural image data. We firstly learn an empirical distribution of the
 212 real distance distribution from training data (the data "RECEPTOR snr 4"). Thus, for each distance
 213 value, we can have its p-value p based on this distribution. Similarly, we set the linkage cost as the
 214 $-\log(p)$. As in [9], each detection is linked to its 3 nearest neighbors in the next frame.

215 3.5 Details of the data

216 The details of the data we experimented on can be found in Table 2 and 3. It includes the numbers
 217 of frames and detections in each video. After combined with different graph design methods, the
 218 out-coming graph sizes are also listed.

219 **References**

- 220 [1] Ravindra K Ahuja, Thomas L Magnanti, and James B Orlin. Network flows: Theory, algorithms,
221 and applications. 2008.
- 222 [2] Visesh Chari, Simon Lacoste-Julien, Ivan Laptev, and Josef Sivic. On pairwise costs for network
223 flow multi-object tracking. In *Proceedings of the IEEE Conference on Computer Vision and*
224 *Pattern Recognition*, pages 5537–5545, 2015.
- 225 [3] Pedro F Felzenszwalb, Ross B Girshick, David McAllester, and Deva Ramanan. Object detection
226 with discriminatively trained part-based models. *IEEE transactions on pattern analysis and*
227 *machine intelligence*, 32(9):1627–1645, 2009.
- 228 [4] Andrew V Goldberg. An efficient implementation of a scaling minimum-cost flow algorithm.
229 *Journal of algorithms*, 22(1):1–29, 1997.
- 230 [5] Harold W Kuhn. The hungarian method for the assignment problem. *Naval research logistics*
231 *quarterly*, 2(1-2):83–97, 1955.
- 232 [6] Philip Lenz, Andreas Geiger, and Raquel Urtasun. Followme: Efficient online min-cost flow
233 tracking with bounded memory and computation. In *Proceedings of the IEEE International*
234 *Conference on Computer Vision*, pages 4364–4372, 2015.
- 235 [7] Hamed Pirsiavash, Deva Ramanan, and Charless C Fowlkes. Globally-optimal greedy algorithms
236 for tracking a variable number of objects. In *CVPR 2011*, pages 1201–1208. IEEE, 2011.
- 237 [8] Sarthak Sharma, Junaid Ahmed Ansari, J Krishna Murthy, and K Madhava Krishna. Beyond
238 pixels: Leveraging geometry and shape cues for online multi-object tracking. In *2018 IEEE*
239 *International Conference on Robotics and Automation (ICRA)*, pages 3508–3515. IEEE, 2018.
- 240 [9] Shaofei Wang, Steffen Wolf, Charless Fowlkes, and Julian Yarkony. Tracking objects with
241 higher order interactions via delayed column generation. In *Artificial Intelligence and Statistics*,
242 pages 1132–1140, 2017.
- 243 [10] Xiaoyu Wang, Ming Yang, Shenghuo Zhu, and Yuanqing Lin. Regionlets for generic object
244 detection. In *Proceedings of the IEEE international conference on computer vision*, pages
245 17–24, 2013.
- 246 [11] Li Zhang, Yuan Li, and Ramakant Nevatia. Global data association for multi-object tracking
247 using network flows. In *2008 IEEE Conference on Computer Vision and Pattern Recognition*,
248 pages 1–8. IEEE, 2008.